AD-A102 414   CAMBRIDGE UNIV (ENGLAND) CAVENDISH LAB   F/G 20/4
VORTEX SHEDDING FREQUENCIES FOR A CYLINDER IN CONFINED FLOW.(U)
MAR 81 W G REES, W A WILBY   AFOSR-79-0057

UNCLASSIFIED   AFOSR-TR-81-0598   NL

1 OF 1
AD A
102414

END
DATE
FILMED
8-81
DTIC

VORTEX SHEDDING FREQUENCIES FOR A CYLINDER IN CONFINED FLOW

W. G. REES

W. A. WILBY

Physics and Chemistry of Solids Group,
Cavendish Laboratory,
University of Cambridge,
Cambridge CB3 OHE

AFOSR-79-0057

SECURITY CLASSIFICATION OF THIS PAGE (When Data Entered)

REPORT DOCUMENTATION PAGE

READ INSTRUCTIONS BEFORE COMPLETING FORM

1. REPORT NUMBER: AFOSR-TR-81-0598
2. GOVT ACCESSION NO.: AD-A102 414
3. RECIPIENT'S CATALOG NUMBER
4. TITLE (and Subtitle): VORTEX SHEDDING FREQUENCIES FOR A CYLINDER IN CONFINED FLOW
5. TYPE OF REPORT & PERIOD COVERED: INTERIM MARCH 1981
6. PERFORMING ORG. REPORT NUMBER
7. AUTHOR(s): W. G. REES, W. A. WILBY
8. CONTRACT OR GRANT NUMBER(s): AFOSR-79-0057
9. PERFORMING ORGANIZATION NAME AND ADDRESS: UNIVERSITY OF CAMBRIDGE, PHYSICS AND CHEMISTRY OF SOLIDS GROUP, CAMBRIDGE CB3 OHE
10. PROGRAM ELEMENT, PROJECT, TASK AREA & WORK UNIT NUMBERS: 2307/A2, 61102F
11. CONTROLLING OFFICE NAME AND ADDRESS: AIR FORCE OFFICE OF SCIENTIFIC RESEARCH/NA, BUILDING 410, BOLLING AFB, DC 20332
12. REPORT DATE: 10 MARCH 1981
13. NUMBER OF PAGES: 19
14. MONITORING AGENCY NAME & ADDRESS (if different from Controlling Office)
15. SECURITY CLASS. (of this report): UNCLASSIFIED
15a. DECLASSIFICATION/DOWNGRADING SCHEDULE

16. DISTRIBUTION STATEMENT (of this Report)

Approved for public release; distribution unlimited.

17. DISTRIBUTION STATEMENT (of the abstract entered in Block 20, if different from Report)

18. SUPPLEMENTARY NOTES

19. KEY WORDS (Continue on reverse side if necessary and identify by block number)

VORTEX SHEDDING
MAGNETOMETER
FREQUENCY MEASUREMENT
VIBRATION

20. ABSTRACT (Continue on reverse side if necessary and identify by block number)

Measurements are presented of vortex shedding frequencies for circular cylinders in confined flows. Experiments have been performed at Reynolds numbers up to 20,000. The range of blockage ratios covered was 0.18-0.33. Systematic changes in the shedding frequency were observed with increasing blockage, the effect being greatest at Reynolds numbers of a few thousand. Measurements of the Reynolds number for which vortex shedding just begins show that the confining walls increase the stability of the flow round the cylinder. The shedding frequency was determined using constant temperature hot wire anemometry, and also using

the vibration response of a magnetometer, a method which, we feel, offers some advantages over conventional techniques.

Accession For	
NTIS GRA&I	☒
DTIC TAB	☐
Unannounced	☐
Justification	
By	
Distribution/	
Availability Codes	
Dist	Avail and/or Special
A	

SUMMARY

Measurements are presented of vortex shedding frequencies for circular cylinders in confined flows. Experiments have been performed at Reynolds numbers up to 20,000. The range of blockage ratios covered was 0.18-0.33. Systematic changes in the shedding frequency were observed with increasing blockage, the effect being greatest at Reynolds numbers of a few thousand. Measurements of the Reynolds number for which vortex shedding just begins show that the confining walls increase the stability of the flow round the cylinder.

The shedding frequency was determined using constant temperature hot-wire anemometry and also using the vibration response of a magnetometer, a method which, we feel, offers some advantages over conventional techniques.

INTRODUCTION

The shedding frequency of vortices from a circular cylinder, corresponding to the frequency of the fluctuating component of the lift and half that of the drag, is of obvious interest in engineering. While an extensive study has been made of this aspect of fluid dynamics for an ideal unconfined flow, little information exists on the effect of blockage on shedding frequencies.

As windtunnel tests and engineering problems may involve significant blockage of the flow, this effect is of some importance. This is particularly true in the case of a high degree of confinement, where large deviations from predictions for unconfined flow are observed.

Our interest in this problem arose from measurements on electromagnetic radiation from turbulent gas flows (see Clark[1]). In an attempt to detect electromagnetic radiation from vortices in the flow, a small magnetometer was mounted in the wall of a "perspex" (PMMA) windtunnel, above a cylinder which spanned the test section. The magnetometer was found to respond to vibration of the windtunnel wall caused by the pressure fluctuations near the cylinder [2]. The dominant frequency of the signal corresponded to the vortex shedding frequency (typically about 20 kHz). The observed deviations from the accepted results for vortex shedding frequencies (Schlichting [3]) were considered to be a consequence of the high degree of confinement, or windtunnel blockage (33% in these tests).

A literature search for corresponding data revealed little information on this problem. Accordingly, the present programme of research was initiated with the aims of establishing the use of the magnetometer in the measurement of shedding frequencies, and of obtaining shedding frequency data for a range of blockage ratios and Reynolds Numbers.

EXPERIMENTAL ARRANGEMENT AND INSTRUMENTATION

This work was performed using a miniature "perspex" (PMMA) windtunnel, producing flow with low turbulence levels. The tunnel runs using air from an Ingersoll Rand compressor, producing up to 2 m^3/min at 700 kPa. The pressurised gas is fed via pressure regulators (usually two in series to minimise the effect of inlet pressure changes on flow rate) into a turbulence suppressor tank. This cylindrical copper tank contains a honeycomb array of 1400 thin walled glass tubes (ca 0.46m in length and 5mm i/d) and two screens of 100 mesh stainless steel. A fairing then guides the air into a rectangular stagnation section, measuring 51mm x 126mm. A smooth two stage contraction then reduces the cross-sectional area of the flow to 5mm x 20mm, the size of the test section, over a distance of 0.3m. (See fig. 1).

The maximum channel Reynolds number attainable is about 50,000. Cylinders of differing diameters can be mounted across the centre of the test section, at a point 120mm downstream of the contraction, and 90mm upstream of the exit of the tunnel.

The cyliners used in measurements of vortex shedding frequencies were a 1.63mm diameter hollow brass cylinder (blockage ratio d/h=0.33), a 1.17mm diameter copper wire (d/h=0.24) and a 0.89mm diameter copper wire (d/h=0.18).

The flow velocity in the test section was determined using a precision dial manometer, or a 25 degree tilt paraffin manometer, connected to a static tap in the stagnation section. For very low flow velocities a fixed flow rate was established, and the flow velocity measured directly, in the absence of a cylinder, using the hot-wire anemometer. The range of cylinder Reynolds numbers covered was approximately 100 - 20,000.

The constant temperature hot-wire anemometer used was constructed by the Fluid Dynamics Group at the Cavendish Laboratory. The hot-wire was 2.5μ m in diameter and was operated at an overheat ratio of 1.50. AC signals from the anemometer were fed to a Marconi Instruments TF2370 Spectrum Analyser and to a cathode ray oscilloscope. The hot-wire probe was 3mm in dia and was aligned with the centre line of the tunnel.

The probe could be adjusted to give optimum signals, generally with the wire 2 to 5 cylinder diameters downstream from the cylinder, and slightly above or below the centreline. Typical signals are shown in fig. 2 (cf ref. [4]). For low flow speeds the most accurate determination of the shedding frequency could be made using the CRO. For higher speeds the spectrum analyser was used, giving a resolution of a few percent.

The magnetometer used in this work consisted of a 1000 turn solenoid coil wound on a ferrite core, connected via a preamplifier and impedance matching circuit to the spectrum analyser.

The intrinsic frequency response of the magnetometer circuit (i.e. response to a magnetic signal) is plotted in figure 3, and a typical spectrum in fig. 4. The coil measured 16mm x 3.5mm in diameter, and was recessed in the wind-tunnel wall above the cylinder. It was rigidly cemented in place using plaster of paris or beeswax. Vibration amplitudes of the order of a few microns could be detected. Hot-wire anemometer measurements were made up to 30 m/s, the maximum speed possible with this arrangement. Magnetometer measurements were made from 50 to 200 m/s. The fact that, in this case, the upper useful limit on the hot-wire data corresponds to the lower useful limit on the magnetometer data illustrates the complementary use of these two methods, and permits a comparison for intermediate Reynolds numbers.

Using the hot-wire, measurements of critical Reynolds numbers, i.e. those at which shedding just begins, were also made.

These measurements were extended to lower blockages using finer wires (down to 0.19mm dia.). The thinner wires were tensioned across the test section and clamped to ensure that they were straight. They were not used for frequency measurements at higher flow speeds due to doubts about their rigidity.

RESULTS AND DISCUSSION

Plots of the dimensionless shedding frequency (Strouhal number) as a function of cylinder Reynolds number are given in fig. 5. The Strouhal number is given by $St = fd/U_o$ where, in unconfined flow, d is taken to be the cylinder diameter and U_o the undisturbed flow velocity far from the cylinder. The latter concept is obviously not applicable in a confined flow, and we use instead the mean channel flow velocity, U.

The use of a reduced or universal Strouhal number is advocated by several authors (Roshko [5], Richter and Naudascher [6], and others). This involves a description of the shedding in terms of the wake parameters. The reduced Strouhal number is given by $St^* = fd'/U_s$ and the Reynolds number by $Re^* = U_s d'/\nu$ where d' is the width of the wake and U_s the separation velocity. In the heavily confined flow used in this work we take d' = d and U_s to be the mean velocity between the cylinder and the wall. Taking account of the lower wake drift velocity U_s can then be calculated from static pressure measurements. While these approximations would be unacceptable for low blockages, they are correct in the limit of high blockages.

The mean flow velocity, U, is then calculated using the continuity equation

$$U = U_s\,(1 - d/h)$$

(see fig. 6).

Figure 7 shows a plot of the critical Reynolds number as a function of the blockage ratio. It can be seen that this rises rapidly with increasing flow confinement. This can be explained by a reduction in the wake width due to the confining walls. Extrapolation to zero blockage yields a value for the critical Reynolds number for unconfined flow consistent with accepted results (Tritton, [7]).

It is well known that vortex shedding can be significantly influenced by other factors, such as wall boundary layers, free stream turbulence levels, cylinder vibration and cylinder aspect ratio. The effect of the boundary layers in the tunnel, fairly thick in this case, cannot be predicted with great certainty. With increasing confinement or Reynolds number the effect of upstream boundary layer development is expected to become less important. However, a full description of the problem would undoubtedly involve the windtunnel parameters as well as those of the cylinder. With the tunnel design used, free stream turbulence levels will be extremely small, and the blockage will be the dominant factor.

Cylinder vibration should be minimal, the cylinders being small and rigidly fixed to the windtunnel walls. There was no evidence that this might have been a problem.

Changes in cylinder diameter necessarily involved changes in the aspect ratio, l/d, of the cylinder. However, the smallest aspect ratio used was 12.3 at a blockage ratio of 0.33. This should be sufficiently large for blockage to again be the dominant factor (compare with 8.6 in [6]). The calculations of Richter and Naudascher [6] on shedding frequencies at high Reynolds Numbers and blockages should yield similar results to our own and a comparison is made with their measurements and those for zero blockage [3] in figure 8. It can be seen that the agreement is good. Data from Drescher [8] are also presented. These show small deviations from zero blockage data and we think that this may be a consequence of the windtunnel blockage (up to 0.18) and low aspect ratio (down to 4.2) in his experiments.

Good agreement has been obtained, as can be seen from fig. 5, between frequency data using the hot-wire and using the magnetometer. The magnetometer data are somewhat scattered, but it is felt that this method is capable of some refinement. For example, the imposition of a strong inhomogenous magnetic field increases the signal strength considerably, and this approach could lead to better accuracy. The chief advantages of this method of frequency measurement are a good high frequency response, the robustness of the probe and the fact that the probe is not introduced into the flow. With larger cylinders or other test bodies the magnetometer could, of course, be mounted inside the cylinder. As no alteration of the surface of the test object is necessary, it also has advantages over sensors such as piezoelectric elements or hot films.

CONCLUSIONS

Measurements of vortex shedding frequencies for a circular cylinder in a heavily confined flow have been obtained for blockage ratios up to 0.33 and Reynolds numbers up to approx. 20,000. As the blockage ratio is increased, systematic deviations from the accepted results for unconfined flow are observed, these being greatest at Reynolds numbers of about 2,000.

The Reynolds number at which vortex shedding begins increases with blockage coefficient, showing that the confining walls increase the stability of the flow.

Measurements made with the magnetometer show that it is possible to determine shedding frequencies using a probe which is not introduced into or in contact with the fluid.

ACKNOWLEDGEMENTS

The windtunnel and magnetometer were designed by Dr. J. Clark of the Cavendish Laboratory. We acknowledge helpful discussions with Drs. J. E. Field and J. C. Mumford of the Cavendish Laboratory, and with Dr. D. J. Maull of the

Engineering Department, University of Cambridge. The research was supported in part by the Science Research Council with a grant to W.G.R. and by the US Air Force (AFOSR Grant No. 79-0057).

REFERENCES

1. J. Clark, AIAA Journal, 13 (1975) 1332-1384.
2. W. A. Wilby, W. G. Rees and J. E. Field, Cambridge University Physics Dept. Report (November 1980).
3. H. Schlichting, Boundary Layer Theory, McGraw Hill, New York, 7th ed., 1979.
4. L. S. G. Kovasznay, Proc. R. Soc. Lond., A198 (1949) 174-190.
5. A. Roshko, NACA TN 3169 (1954).
6. A. Richter and E. Naudascher, J. Fluid Mech., 78 (1976) 561-576.
7. D. J. Tritton, Physical Fluid Dynamics, Van Nostrand Reinhold, New York, 1st ed., 1979.
8. H. Drescher, Z. Flugwiss., 4(1956) 17-21.

LIST OF CAPTIONS

Fig. 1. Schematic Diagram of Windtunnel System.

Fig. 2a. Typical CRO Signal from hot-wire (low velocity).

2b. Typical Spectrum from hot-wire (high velocity).

Fig. 3. Intrinsic Frequency Response of Magnetometer.
Signal Intensity against frequency.

Fig. 4. Typical Spectrum from Magnetometer.

Fig. 5. Plot of Strouhal number against Reynolds number for different Blockage Ratios.

Fig. 6. Schematic Diagram of Test Section.

Fig. 7. Plot of Critical Reynolds number against Blockage Ratio.

Fig. 8. Curves of Strouhal number against Reynolds number
Oa) from Schlicting [3]
Ob) after Drescher [8]
Other data - present work Re $<2 \times 10^4$
- after Richter & Naudascher [6] Re $>2 \times 10^4$

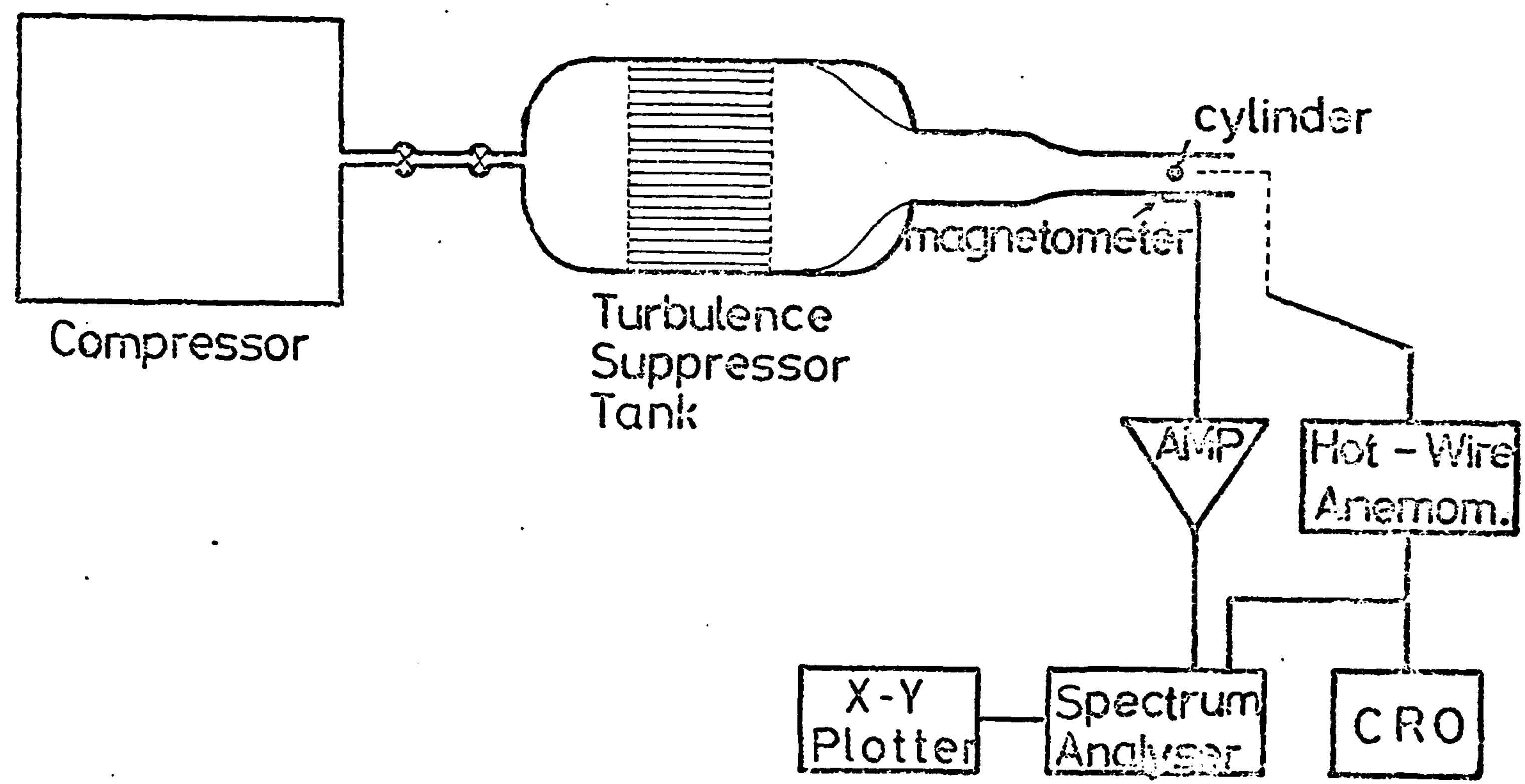
Compressor
Turbulence
Suppressor
Tank
cylinder
magnetometer
AMP
Hot - Wire
Anemom.
X-Y
Plotter
Spectrum
Analyser
CRO

Fig 1

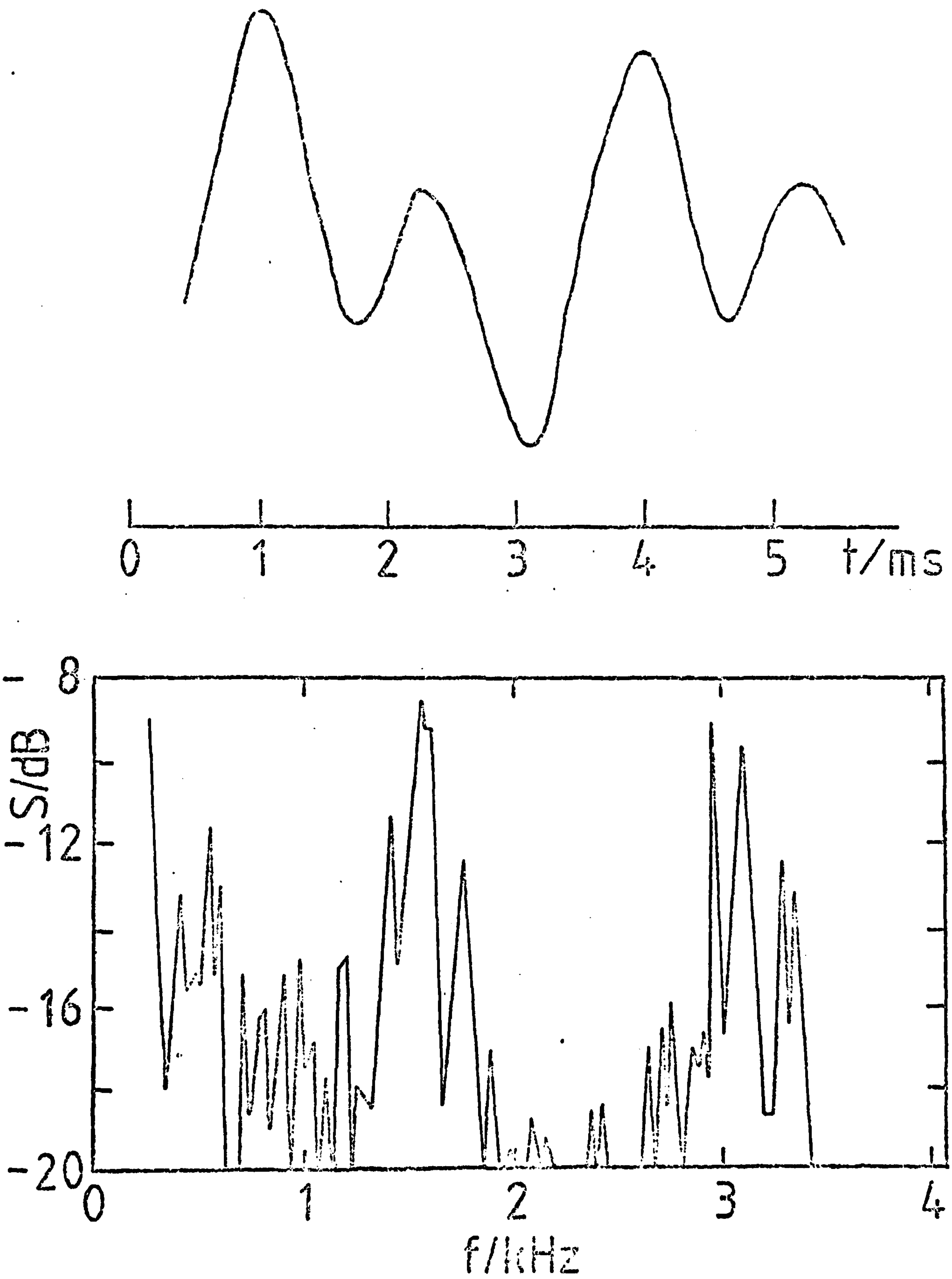

fig 2

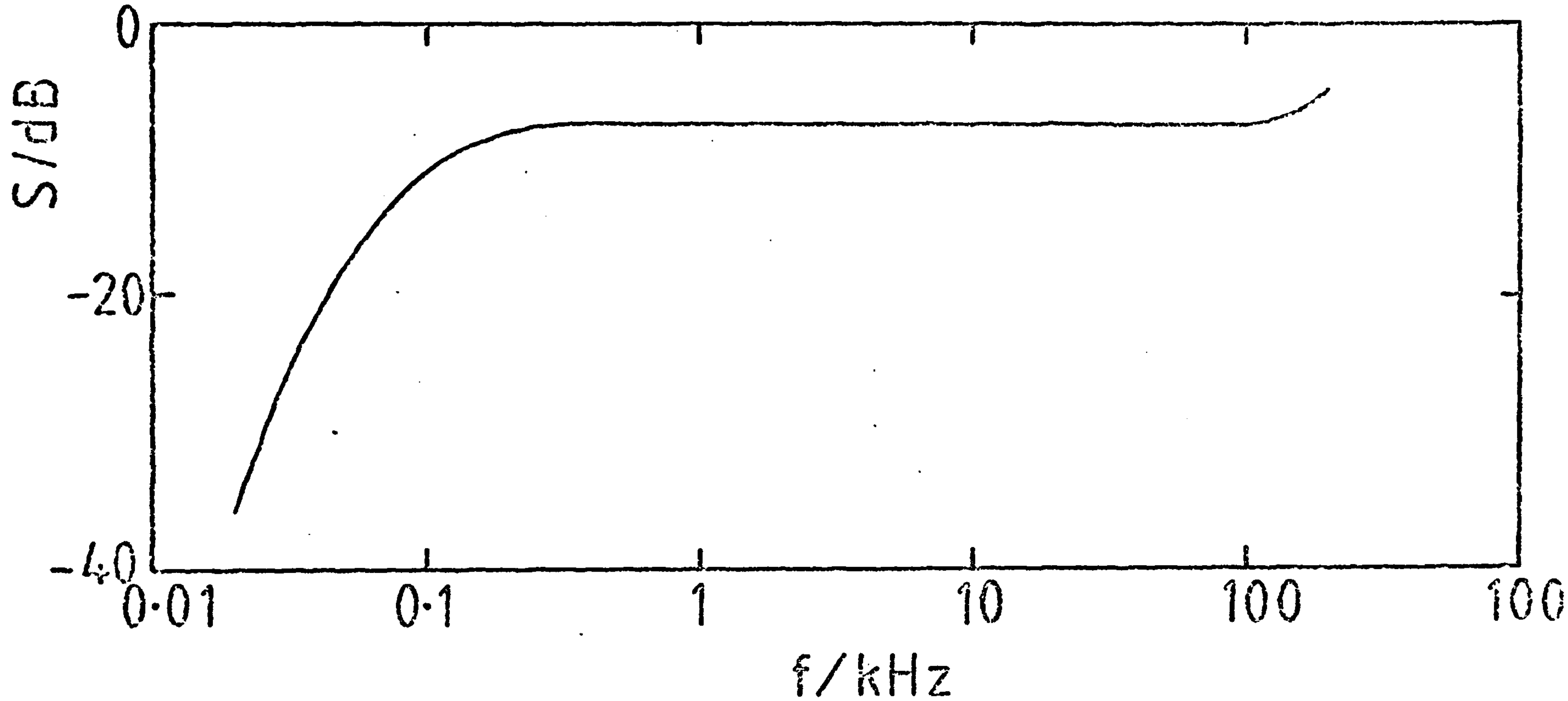

fig 3

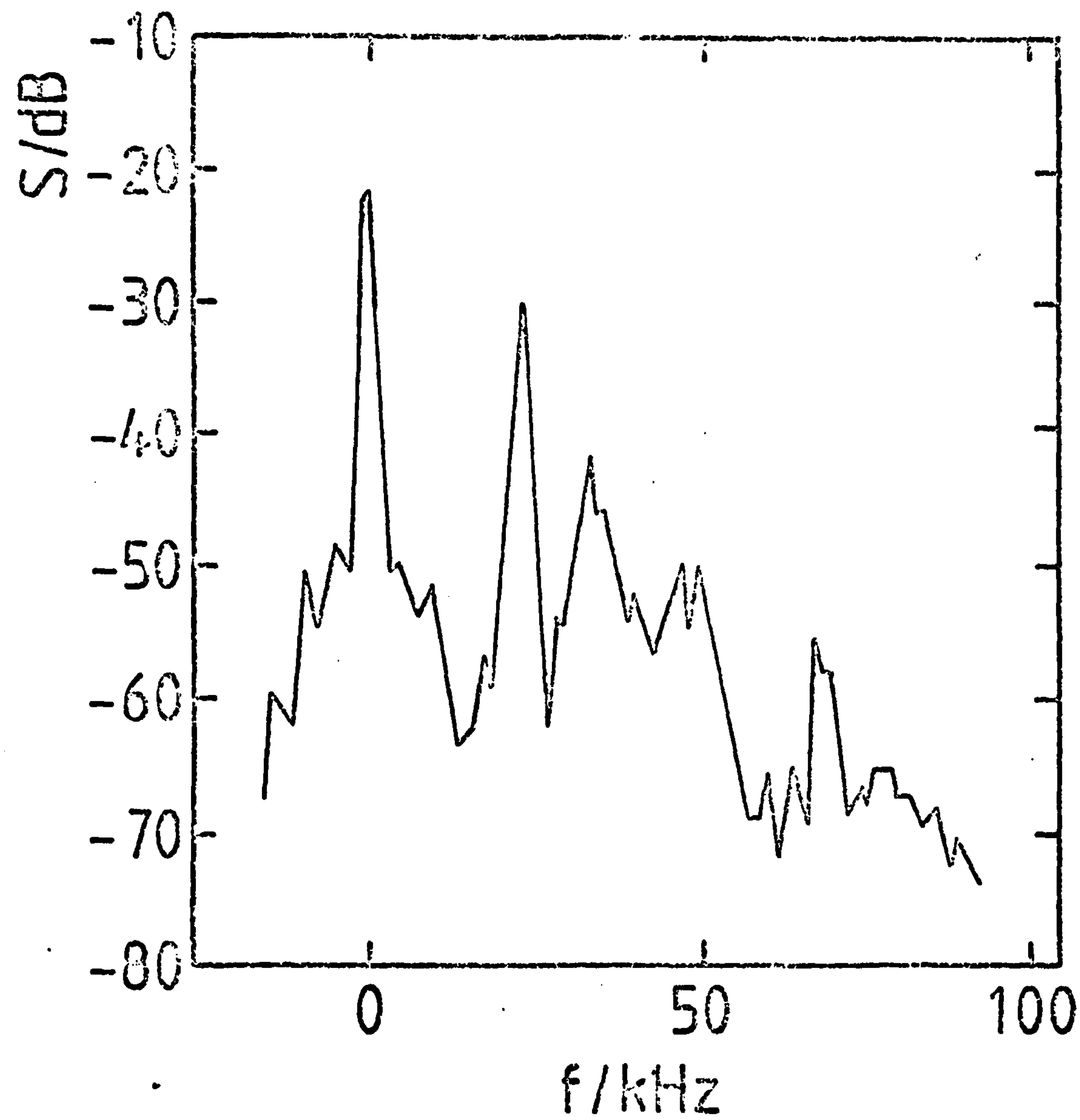

fig 4

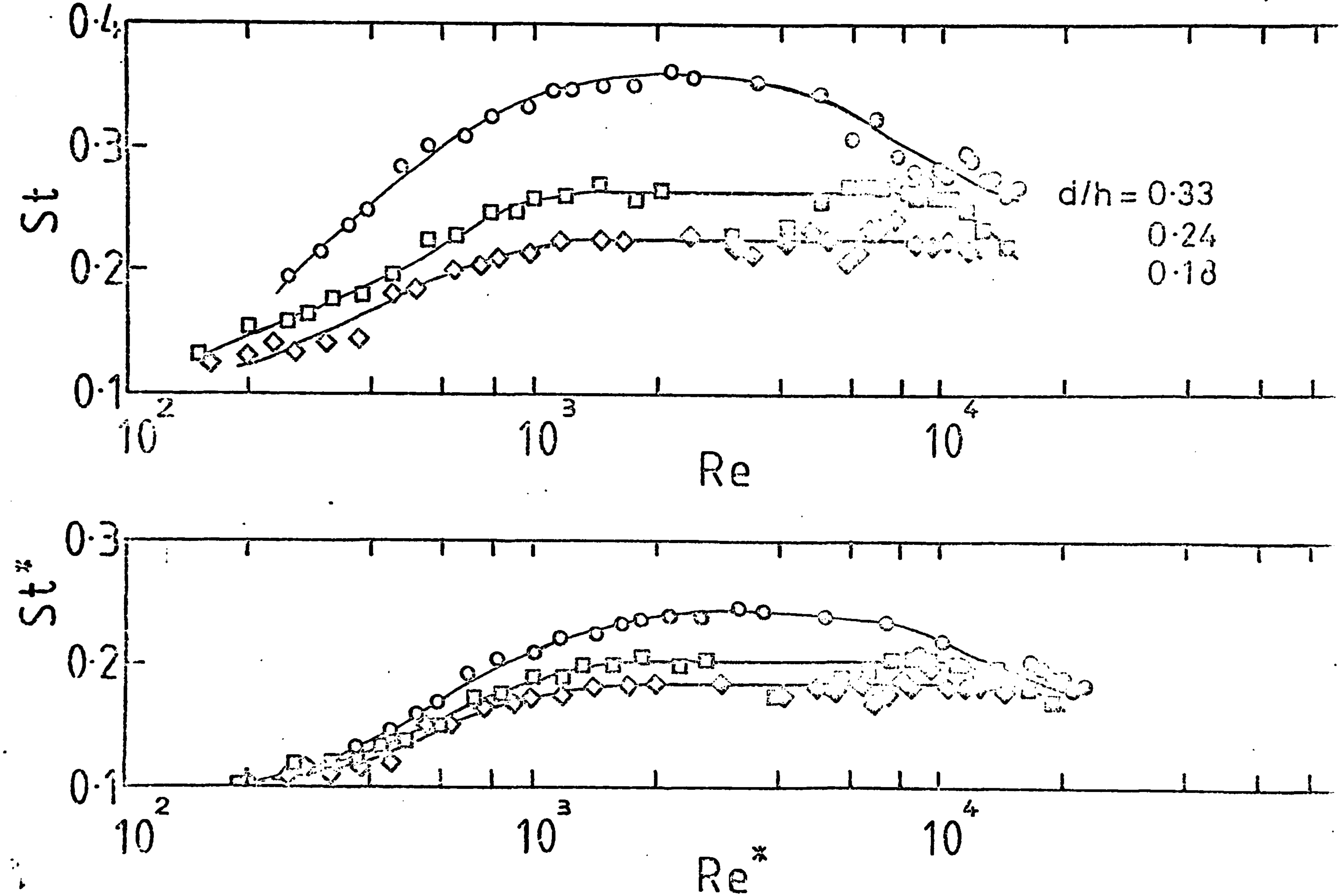
St
0·4
0·3
0·2
0·1
d/h = 0·33
0·24
0·18
10^2
10^3
10^4
Re
St*
0·3
0·2
0·1
10^2
10^3
10^4
Re*

fig 5

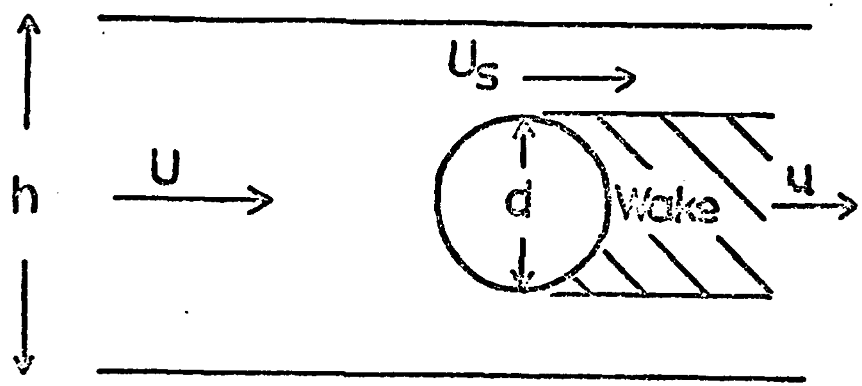

fig 6

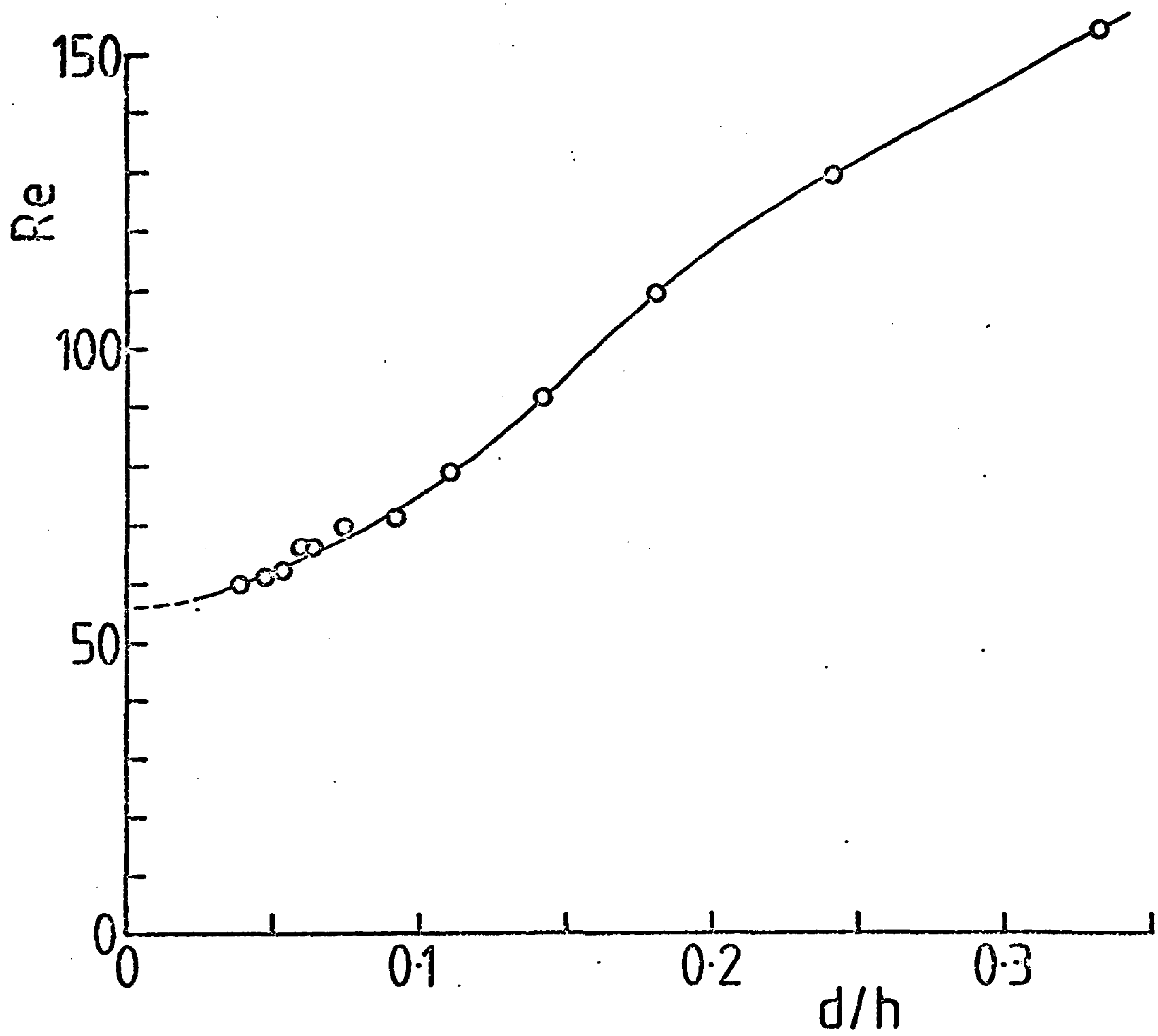

Fig 7

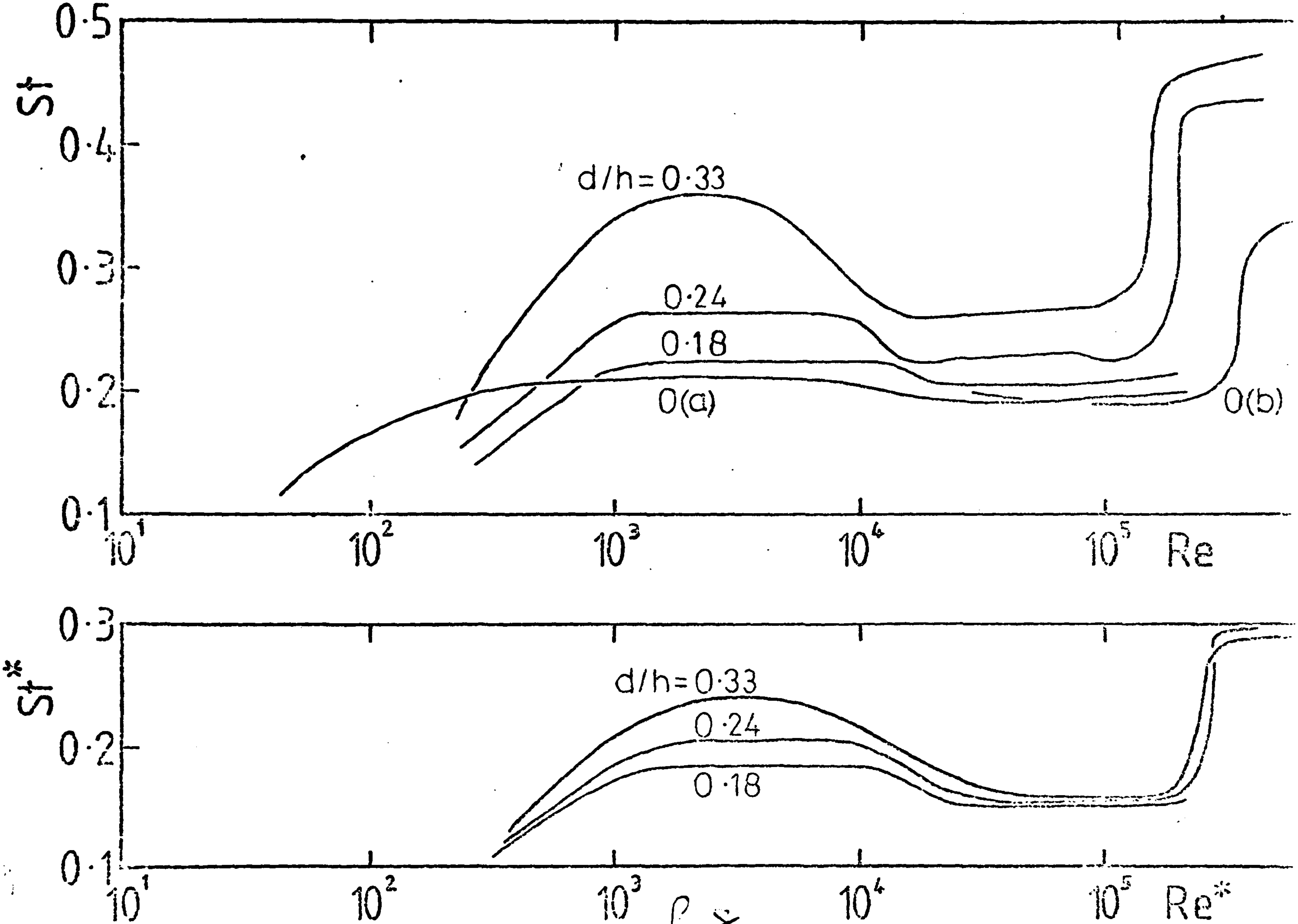
St
0·5
0·4
0·3
0·2
0·1
d/h=0·33
0·24
0·18
0(a)
0(b)
10^1
10^2
10^3
10^4
10^5
Re
St*
0·3
0·2
0·1
d/h=0·33
0·24
0·18
10^1
10^2
10^3
10^4
10^5
Re*

Fig 8